JOURNAL OF SOLID STATE CHEMISTRY **136,** 87–92 (1998)
ARTICLE NO. SC977662

Synthesis, Crystal Structure, and Characterization of the New Ordered Hollandite-Type $NdMo_6O_{12}$

J. Tortelier,* W. H. McCarroll,† and P. Gougeon*,[1]

*Laboratoire de Chimie du Solide et Inorganique Moléculaire, U.R.A. C.N.R.S. n° 1495, Université Rennes I, Avenue du Général Leclerc, 35042 Rennes Cedex, France; and †Department of Chemistry, Rider College, Lawrenceville, New Jersy 08648

Received June 17, 1997; in revised form October 14, 1997, accepted October 20, 1997

Single crystals of $NdMo_6O_{12}$ were prepared by fused-salt electrolysis at 960°C from a melt of Rb_2MoO_4, MoO_3, and Nd_2O_3 having the molar ratio 8.4:5:1. The compound crystallizes in the tetragonal space group $I4/m$ with $a = 9.8988(2)$ Å, $c = 8.6434(5)$ Å, $V = 846.93(5)$ Å^3, and $Z = 4$. The structure of $NdMo_6O_{12}$ has been determined from single-crystal X-ray diffraction data and refined to reliability factors of $R(F_o) = 0.0409$ and $R_w(F_o^2) = 0.0612$ for all the reflections (1282). $NdMo_6O_{12}$ adopts a hollandite-related structure with a tripled c-axis. Within the double chains of edge-sharing MoO_6 octahedra, the Mo atoms form infinite chains of Mo_3 triangular clusters. Another dominant feature of the structure is the ordering of the Nd^{3+} cations within the channels delimited by the Mo–O double strings. $NdMo_6O_{12}$ shows semiconducting behavior along the chains with an activation energy of 0.3 eV and a room-temperature resistivity of 0.49 Ω · cm. The magnetic susceptibility data indicate paramagnetic behavior due to the Nd^{3+} moment at high temperature.

INTRODUCTION

A large number of ternary transition-metal oxides $A_xM_8O_{16}$ (A = K, Rb, Cs, Ba, Pb …; M = Ti, V, Cr, Mn, Fe, Mo, Ru …) which crystallize in the hollandite-type structure have been synthesized by solid state reaction or by fused-salt electrolysis since the first report of the crystal structure of the mineral hollandite $BaMn_8O_{16}$ in 1950 (1). Their structures consist of double rutile chains sharing edges and corners of the MO_6 octahedra and forming one-dimensional square tunnels in which the A cations reside. The great interest aroused by this family of compounds is mainly due to the possibility of one-dimensional ionic conductivity through the tunnel on the one hand, and on the other that they constitute the major phase in SYNROC (2), a synthetic rock used for the storage of radioactive wastes. In addition, these phases frequently exhibit complex commensurate or incommensurate superstructures due to partial occupation and ordering of the A cation within the tunnels. Reduced molybdenum oxides which crystallize with a hollandite-type tunnel structure are also characterized by a clustering of the Mo atoms. This clustering results in the formation of tetrameric molybdenum Mo_4 clusters for the $K_2Mo_8O_{16}$ (3), $Ba_{1.14}Mo_8O_{16}$ (4), $Li_{0.35}BaMo_8O_{16}$ (5), and $Na_{0.35}BaMo_8O_{16}$ (5) compounds synthesized by solid state reaction, and Mo_3 triangles for the $La_{1.16}Mo_8O_{16}$ (6) compound obtained by fused-salt electrolysis. While in $K_2Mo_8O_{16}$ all square-prismatic sites are occupied, a partial occupation and disorder of the large cations occur in the three Ba compounds. For $La_{1.16}Mo_8O_{16}$, a one-dimensional incommensurate modulated structure with a modulation wave vector of $q^* = 0.608\,c^*$ was determined. We report here the synthesis, single-crystal structure determination, and the study of the physical properties of a new reduced ternary oxide of molybdenum which adopts the hollandite-type structure: $NdMo_6O_{12}$.

[1]To whom correspondence should be addressed.

EXPERIMENTAL

Synthesis. The starting reagents used in this synthesis were Rb_2MoO_4, MoO_3 (Strem, 99.9%) and Nd_2O_3 (Strem, 99.997%). Rubidium molybdate was prepared by reacting Rb_2CO_3 (Strem, 99.9%) with a stoichiometric amount of MoO_3 at 600°C overnight. MoO_3 and Nd_2O_3 were ignited in air at 400°C and 800°C, respectively before use. Single crystals of $NdMo_6O_{12}$ were obtained by the electrolysis of a melt formed at 960°C from a mixture of Rb_2MoO_4, MoO_3, and Nd_2O_3 having the molar ratio 8.4:5:1. The electrolysis was carried out in air using an alumina crucible. The anode was a platinum foil with a surface area of about 1 cm^2 and the cathode a spiral platinum made from a 0.4 mm diameter wire. At the end of the run, the electrodes were raised above the melt to allow them to cool rapidly to room temperature. Crystals, which grow perpendicularly to the cathode in black needle-shaped square prisms with the needle axis parallel to the tetragonal c-axis (max. dimensions $0.8 \times 0.8 \times 5$ mm^3), were obtained by applying

0022-4596/98 $25.00

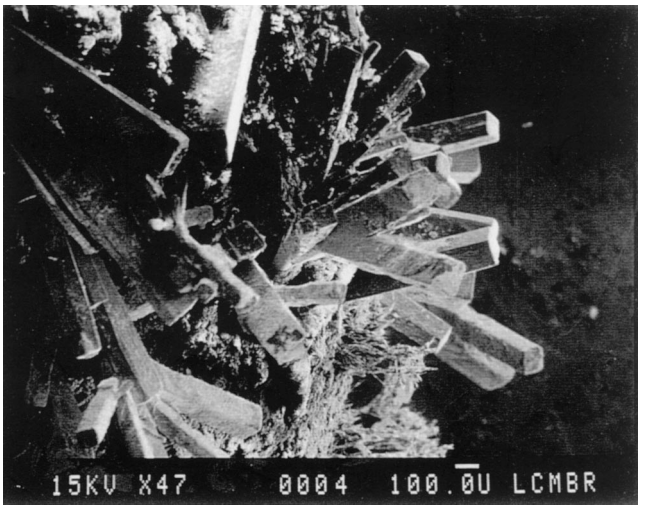

FIG. 1. Crystals of $NdMo_6O_{12}$ deposited on the cathode.

a constant current of 36 mA for 12 h (Fig. 1). Under these conditions, very small amounts of crystals of $Nd_4Mo_{18}O_{32}$, which is isostructural with $Gd_4Mo_{18}O_{32}$ (7), were also produced. Single crystals were separated from the matrix and the cathode by repeated and alternate washings in hot dilute solutions of potassium carbonate and hydrochloric acid. Single crystals of $NdMo_6O_{12}$ and $Nd_4Mo_{18}O_{32}$ were easily separated owing to their different habit. Qualitative microanalyses of the $NdMo_6O_{12}$ crystals thus obtained using a JEOL JSM-35 CF scanning electron microscope equipped with a Tracor energy dispersive-type X-ray spectrometer did not show any elements in concentration above 1% by weight other than the neodymium, molybdenum, and oxygen. In particular, no Si and Al were observed as reported for $La_{1.16}Mo_8O_{16}$ by Leligny *et al.* Indeed, the authors hypothesize that the silicon and the aluminium would tend to promote the growth of single crystals of $La_{1.16}Mo_8O_{16}$ since the latter were obtained only after the crucible had been soaked for several hours in the melt or if some silica was added. In our case, this assumption seems to be challenged since crystals of $NdMo_6O_{12}$ were obtained from the first run with a new high-density alumina crucible as well as a zirconia crucible.

Electrical conductivity and magnetic susceptibility measurements. The dc resistivity measurement was made on a single crystal (dim: $0.82 \times 0.08 \times 0.08\ mm^3$) with a current of 50 nA using a standard four-probe technique between 300 and 77 K. Ohmic contacts were made by attaching gold wires to the crystal with conducting silver paint.

The magnetic studies were performed under a magnetic field of 0.4 T on a batch of randomly oriented single crystals using a SQUID susceptometer (SHE VTS-906) in the range 5–300 K.

Structure determination. A needle-like crystal of approximate dimensions $0.26 \times 0.017 \times 0.015\ mm^3$ was selected for data collection. Intensity data were collected by the ω-2θ scan method on a CAD4 Enraf-Nonius diffractometer using graphite-monochromatized MoKα radiation ($\lambda = 0.71073$ Å) at room temperature. A scan width of $\Delta\omega = (0.80 + 0.35 \operatorname{tg}\theta)^\circ$ and a counter aperture of $\Delta l = (2 + 0.5 \operatorname{tg}\theta)$ mm were used. Three orientation and three intensity control reflections from diverse regions of reciprocal space were checked every 250 reflections and every hour respectively and showed no systematic variations throughout data collection. The raw data were corrected for Lorentz and polarization effects and for absorption by employing the Ψ scan method (8) on six reflections. Examination of the data set did not show any supplementary systematic extinctions other than that corresponding to the I-type lattice and revealed that the Laue class was 4/m leading to space groups $I4$, $I\bar{4}$, or $I4/m$. The lattice constants were determined by least-squares refinement of the setting angles of 25 reflections in the 2θ range 10–34° that had been automatically centered on the diffractometer. The initial positions for the Nd and Mo atoms were determined by direct methods using SHELXS (9) in space group $I4/m$. The O atoms were located from a subsequent difference Fourier synthesis. Full-matrix least-squares refinement on F^2 on all positional and anisotropic atomic displacement parameters including terms for anisotropic extinction was carried out using SHELXL (10). The final refinement converged to $R_w(F_o^2) = 0.0612$ for all reflections and for those 1085 having $F_o^2 > 2\sigma(F_o^2)$ to the conventional reliability factor $R(F_o) = 0.0311$. The largest shift/e.s.d. was < 0.01. Maximum and minimum electron densities in the final difference Fourier map were $+2.79$ and $-2.04\ e \cdot Å^{-3}$ respectively; the final value of g was $9.5(7) \times 10^{-4}$. Refinements of the occupancy factors for the Nd and Mo sites yielded values of 0.996(3), 1.000(2), and 1.003(2) for Nd, Mo(1), and Mo(2), respectively and showed that they are fully occupied. Attempts to refine the structure in the acentric space groups $I4$ and $I\bar{4}$ were unsuccessful and led to negative values of some of the anisotropic displacement parameters. Calculations were performed on a Digital Pentium Celebris 590 FP for the SHELXS and SHELXL-93 programs and on a Digital microVAX 3100 for the MolEN (11) package (data reduction and absorption corrections). Some data collection and refinement parameters are given in Table 1. The final values of the positional parameters, isotropic-equivalent atomic displacement parameters, and their standard uncertainties are reported in Table 2. Selected interatomic distances are given in Table 3.

STRUCTURAL DESCRIPTION AND DISCUSSION

$NdMo_6O_{12}$ crystallizes in a hollandite-type one-dimensional tunnel structure with a tripled *c*-axis. Such a tripling

TABLE 1
Crystallographic and Experimental Data for $NdMo_6O_{12}$

Formula	$NdMo_6O_{12}$
Molecular weight	911.88
Crystal system	tetragonal
Space group	$I4/m$
a (Å)	9.8988(2)
c (Å)	8.6434(5)
V (Å)	846.93(5)
Z	4
Density (calc., g.cm^{-3})	7.152
Temperature (K)	293
Diffractometer	Enraf-Nonius CAD4
Radiation	Mo$K\alpha$ radiation ($\lambda = 0.71073$ Å)
Crystal color	Black
Morphology	needle
Crystal size (mm^3)	$0.26 \times 0.017 \times 0.015$
Linear absorption coeff. (mm^{-1})	14.684
Monochromator	Oriented graphite
Scan mode	θ–2θ
Recording range 2θ (°)	2–80
hkl range	−12/17, −17/12, 0/12
No. of measured reflections	2596
No. of independent reflections	1282
No. of observed reflections with $F^2 > 2\sigma(F^2)$	1085
Rint	0.024
Absorption correction	ψ scan
Transmission (min.-max.)	0.944–1.000
Refinement	F^2
Calculated weights	$w = 1/[\sigma^2(F_o^2) + (0.0228P)^2 + 0.00440P]$ where $P = (F_o^2 + 2F_c^2)/3$
Extinction coefficient	0.00095(7)
$R[F^2 > 2\ \sigma(F^2)]$	0.0311
$wR(F)$ on all data	0.0409
$wR(F^2)$ on all data	0.0612
S (all data)	1.152
No. of refined parameters	50

of the short axis has already been found, for example, for $BaRu_6O_{12}$ (12), which crystallizes in the space group $P4/n$. The Mo–O framework of $NdMo_6O_{12}$ consists of double-rutile chains of edge-sharing MoO_6 octahedra with each octahedron sharing four edges with four other neighboring octahedra. These double strings, which run parallel to the c-axis, are then linked together by sharing sp^2-type oxygen-atom corners to form large square tunnels in which the

TABLE 2
Fractional Atomic Coordinates and Equivalent Isotropic Displacement Parameters (Å), Calculated as One-third Trace U, for $NdMo_6O_{12}$

Atom	x	y	z	U_{eq}
Nd	0.0000	0.0000	−0.20672(5)	0.00732(8)
Mo(1)	0.33980(3)	−0.81609(3)	−0.34016(4)	0.00617(7)
Mo(2)	0.33374(4)	−0.81544(4)	0.0000	0.00497(8)
O(1)	0.4567(2)	−0.1702(3)	−0.3324(3)	0.0066(4)
O(2)	0.1711(3)	−0.1295(3)	−0.3331(3)	0.0087(5)
O(3)	0.4618(4)	−0.1627(4)	0.0000	0.0070(6)
O(4)	0.1226(4)	0.1606(4)	0.0000	0.0062(6)

TABLE 3
Selected Interatomic Distances for $NdMo_6O_{12}$

Mo(1)–Mo(2)	2.5603(4)	Mo(2)–O(1) (×2)	2.014(2)
Mo(1)–Mo(1)	2.7022(6)	Mo(2)–O(3)	2.035(4)
Mo(1)–Mo(1)	2.7631(7)	Mo(2)–O(2) (×2)	2.063(3)
Mo(1)–Mo(2)	2.9408(4)	Mo(2)–O(4)	2.103(4)
Mo(1)–O(3)	1.998(3)	Nd–O(2) (×4)	2.389(3)
Mo(1)–O(1)	2.020(2)	Nd–O(4) (×4)	2.682(3)
Mo(1)–O(1)	2.042(2)		
Mo(1)–O(2)	2.086(3)		
Mo(1)–O(2)	2.096(3)		
Mo(1)–O(4)	2.101(3)		

Nd^{3+} ions are located (Fig. 2) and smaller-sized channels similar to those found in the rutile-type structure.

While in $BaRu_6O_{12}$, only weak metal-metal interactions are expected due to Ru–Ru distances ranging from 2.91 to 3.13 Å compared to 2.65 Å in Ru metal, strong Mo–Mo interactions, which lead to a clustering of the Mo atoms, are observed in the reduced molybdenum oxides having a hollandite-related structure. Thus tetrameric molybdenum Mo_4 clusters (Fig. 3a) with intracluster distances ranging between 2.53 and 2.84 Å and intercluster distances greater than 3 Å are observed in the $Ba_{1.14}Mo_8O_{16}$, $K_2Mo_8O_{16}$, $Li_{0.35}BaMo_8O_{16}$, and $Na_{0.35}BaMo_8O_{16}$ compounds, while in $La_{1.16}Mo_8O_{16}$, which presents a one-dimensional

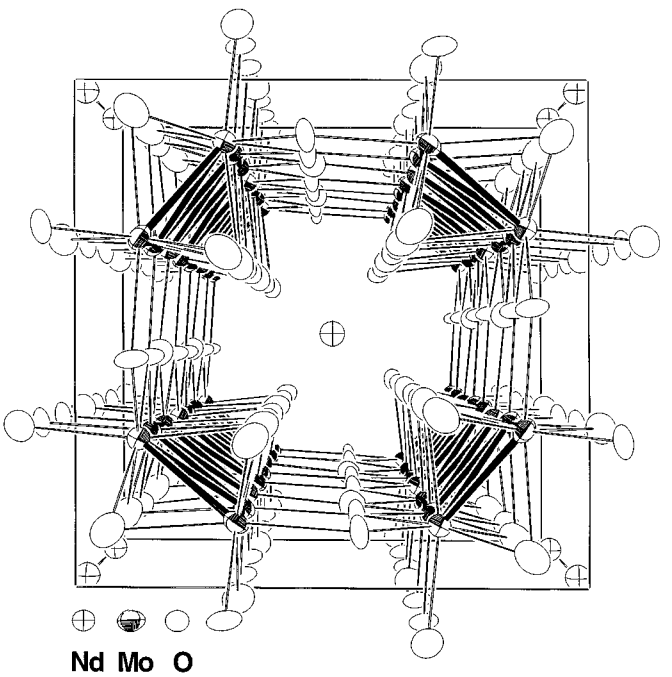

FIG. 2. View of the $NdMo_6O_{12}$ structure along the tetragonal c-axis. Displacement ellipsoids are drawn at the 97% probability level.

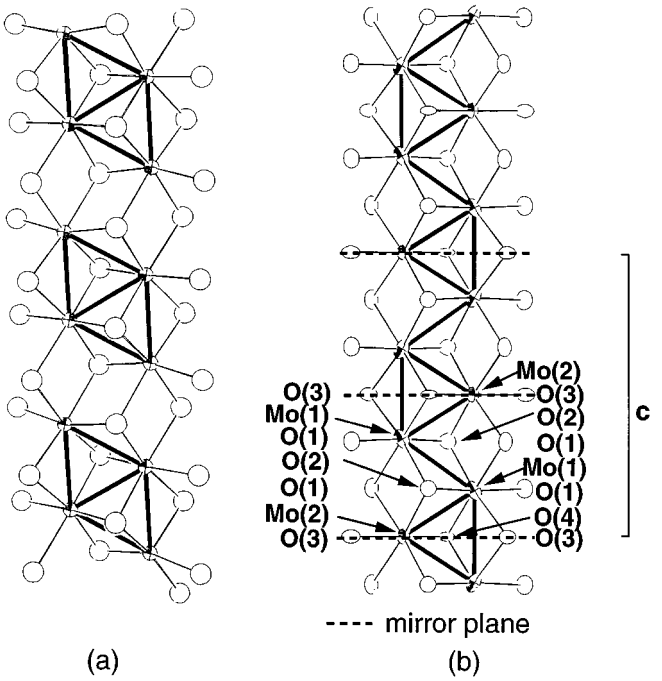

FIG. 3. Sections of the metal-oxide chains in (a) $K_2Mo_8O_{16}$ and (b) $NdMo_6O_{12}$. Mo–Mo bonds are represented by solid black lines.

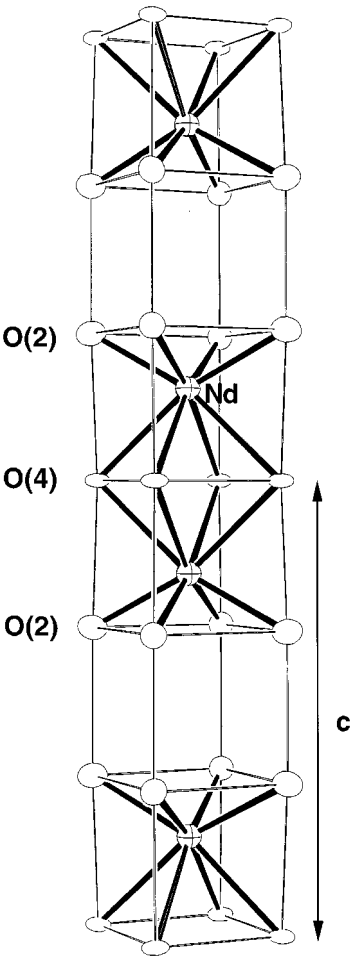

FIG. 4. A view perpendicular to the *c*-axis of $NdMo_6O_{12}$ showing the ordered arrangement of the Nd^{3+} cations within a channel.

incommensurate modulated structure, Mo_3 triangles occur. In $NdMo_6O_{12}$, we observed the formation of infinite metallic chains based on Mo_3 triangular clusters as shown in Fig. 3b. These chains probably result from the lower valence state of the molybdenum $+3.5$ in the Nd hollandite-type compound compared to 3.71–3.75 for the hollandites with Mo_4 clusters. The Mo–Mo distances within the Mo_3 triangles are 2.5603(4) Å for the two diagonal bonds Mo(1)–Mo(2) and 2.7631(7) Å for the Mo(1)–Mo(1) bond parallel to the *c*-axis. The shortest distance between triangles is 2.7022(6) Å and corresponds to the diagonal bond Mo(1)–Mo(1). The other two intertriangle Mo(1)–Mo(2) distances parallel to the *c*-axis are 2.9408(4) Å and thus are only weakly bonding. As previously observed in the other hollandite-related reduced molybdenum oxides, the oxygen atoms can be divided into two different types: O(1) and O(3), which interconnect the double chains and are linked in trigonal planar-like coordination to three Mo atoms, and O(2) and O(4), which bridge three Mo atoms of the same double chain and are also bonded to one [O(2)] or two Nd atoms [O(4)]. The Mo–O bond lengths vary from 1.998(3) to 2.042(2) Å for the oxygen atoms of the former type and from 2.063(3) to 2.103(4) Å for those of the second type. From the Mo–O bond lengths, the valences of the two crystallographically independent Mo atoms calculated by using the relationship of Brown and Wu [$(s = (d_{Mo-O}/1.882)^{-6.0})$] (13) are $+3.54(3)$ and $+3.62(3)$, respectively. This yields an average value of $+3.57(3)$, in reasonably good agreement with the expected value of $+3.5$.

The Nd^{3+} ions occupy, in an ordered way, two out of the three possible square-prismatic sites formed by the intrachain oxygen atoms as observed in $BaRu_6O_{12}$ (Fig. 4). On the other hand, it should also be mentioned that such a cationic sequence has been proposed for $K_{1.33}Mn_8O_{16}$ (14). However the occurrence for this compound of diffuse streaks corresponding to the reciprocal distance $c^*/3$ on the X-ray rotation photographs indicates that the order in a given channel is not correlated with those in adjacent channels. In order to minimize Nd^{3+}–Nd^{3+} Coulomb repulsions in $NdMo_6O_{12}$, the Nd^{3+} ions of two consecutive sites are shifted away from one another along the [001] direction as observed previously for the Ba^{2+} cations in $BaRu_6O_{12}$ and for $La_{1.16}Mo_8O_{16}$ in the regions where La^{3+}–La^{3+} pairs occur. As a consequence, each Nd^{3+} ion is displaced by 0.347 Å from the center of its tetragonal prismatic site and thus has four nearest oxygen atoms at

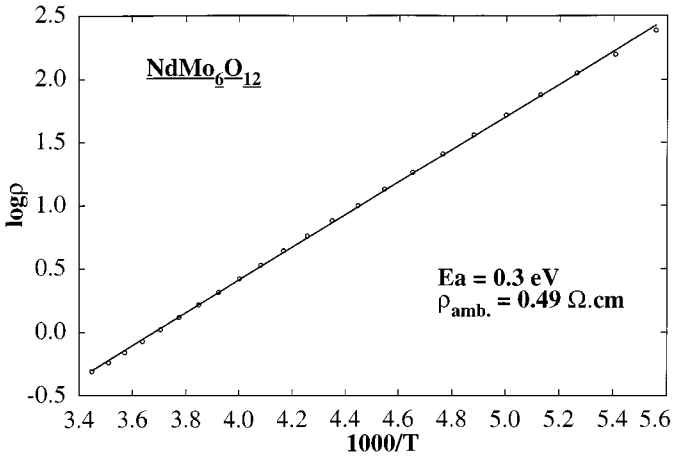

FIG. 5. Arrhenius plot for $NdMo_6O_{12}$.

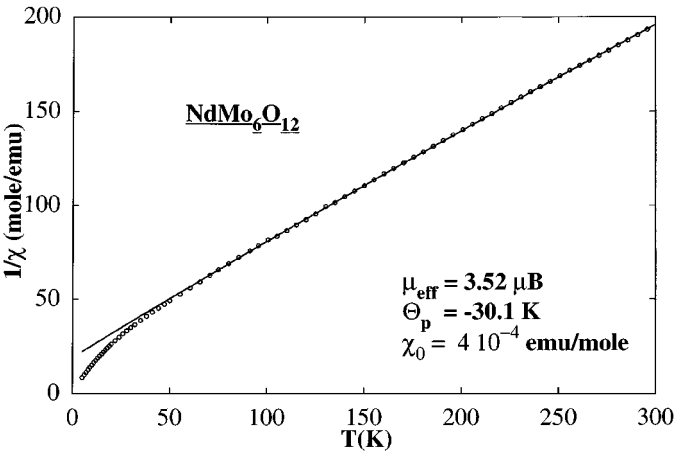

FIG. 6. Magnetic susceptibility of $NdMo_6O_{12}$ crystals as a function of temperature.

2.389(3) Å and four furthest ones at 2.682(3) Å. The average Nd–O bond distance is 2.535 Å, slightly larger than the value 2.50 Å expected from the sum of the ionic radii of Nd^{3+} (CN 8) and O^{2-} (CN 4) (15). The distance between the two close Nd^{3+} ions is 3.5735(9) Å. In comparison, the shortest La^{3+}–La^{3+} distances occuring with the largest probability in $La_{1.16}Mo_8O_{16}$ are 3.72–3.75 Å and between the Ba^{2+} cations in $BaRu_6O_{12}$, 3.86 Å.

The temperature dependence of the electrical resistivity measured along the *c*-axis (direction of the chain of the Mo_3 triangles) (Fig. 5) shows that $NdMo_6O_{12}$ is semiconducting in the temperature range 175–300 K. The resistance below 175 K is greater than 2 MΩ, which is beyond the detection limit of our instrumentation. The room-temperature resistivity is 0.49 Ω · cm and the activation energy calculated in the region 175–300 K is 0.3 eV.

A plot of the inverse of the magnetic susceptibility of $NdMo_6O_{12}$ vs temperature is shown in Fig. 6. The data can be least-squares fit to a modified Curie–Weiss law $\chi = C/(T-\theta) + \chi_0$ over the temperature interval 40–300 K where $C = 1.55\,\text{emu}\cdot\text{K/mole}$, $\theta = -30.1\,\text{K}$ and $\chi_0 = 4.01 \times 10^{-4}\,\text{emu/mole}$. The value of $\mu_{\text{eff.}} = 3.52\,\mu\text{B}$ thus found agrees well with the free-ion value of trivalent neodymium ($\mu_{\text{th}} = 3.62\,\mu\text{B}$). However, given that the average valence of Mo in this compound is 3.5 or 15 electrons per Mo_6 unit, one might have expected to see some contribution from the d electrons of Mo to the observed magnetic moment. Triangular clusters of Mo have been shown to be particularly stable for 6 electrons but can accommodate up to 8 electrons (16). Bond length-bond strength calculations for the metal-metal bonds (17, 18) lead to values of 0.71 and 0.28 electrons for the Mo(1)–Mo(1) and Mo(1)–Mo(2) intercluster distances. This would leave 6.5 electrons per Mo_3 cluster or one unpaired electron for every two clusters, resulting in a small but nonetheless observable, contribution to the total magnetic moment. It would thus appear that this often useful localized model is not applicable in this case and that some sort of a band system applies which can accommodate the 60 electrons per unit cell in 30 two-electron bands. A similar situation has been noted in $La_3Mo_4SiO_{14}$, which is also semiconducting and contains isolated Mo_2 and Mo_3 clusters, and displays an extremely weak paramagnetism of the Van Vleck type (19). Actually, the magnetic behavior and the electronic distribution would be well explained if the repeat unit were doubled (Mo12). The anisotropic displacement of the Mo(1) atom, slightly higher along the *c*-axis suggests some disorder. The latter could be due to such doubled clusters, which would be disordered from one chain to the adjacent ones to give the average result we observed. Unfortunately, long-exposure oscillation photographs around *c* did not reveal any superlattice reflection or diffuse-scattering streak that could confirm such a disorder. Additional studies by a combination of EXAFS and total neutron scattering as used previously for Li_2MoO_3, $LiMoO_2$, and $Li_4Mo_3O_8$ (20, 21) would be helpful to resolve this problem.

In summary, millimeter-size crystals of the new reduced molybdenum oxide $NdMo_6O_{12}$, which crystallizes with a hollandite-related structure, have been grown by molten salt electrolysis. The dominant features of the crystal structure are the formation of infinite chains based on Mo_3 triangles within the Mo_6O_{12} double rutile chains and the ordering of the Nd^{3+} cations with the sequence Nd^{3+}–Nd^{3+}–□ within the square channels. In addition the Nd^{3+} cations are shifted toward the empty sites to minimize the electrostatic repulsions. $NdMo_6O_{12}$ exhibits semiconductor behavior and paramagnetic behavior due to the Nd^{3+} cations. Attempts to synthesize isostructural compounds with other rare earths are in progress. Indeed, cations with different radii could lead to different stoichiometries and orderings of the cations within the channel. In addition, band structure calculations would be

helpful to understand the different kinds of clustering observed in the reduced molybdenum hollandite-type structures and their physical properties.

ACKNOWLEDGMENT

We thank Dr. H. Noël for the collection of the magnetic susceptibility data.

REFERENCES

1. A. Byström and A. M. Byström, *Acta Crystallogr.* **3,** 146 (1950).
2. A. E. Ringwood, S. E. Kesson, N. G. Ware, W. Hibberson, and A. Major, *Nature* **278,** 219 (1979).
3. C. C. Torardi and J. C. Calabrese, *Inorg. Chem.* **23,** 3281 (1984).
4. C. C. Torardi and R. E. McCarley, *J. Solid State Chem.* **37,** 393 (1981).
5. K. H. Lii, Ph.D. thesis, Iowa State University (1985).
6. H. Leligny, Ph. Labbé, M. Ledésert, B. Raveau, C. Valdez, and W. H. McCarroll, *Acta Crystllogr. Sect. B* **48,** 134 (1992).
7. P. Gougeon, P. Gall, and R. E. Mc Carley, *Acta Crystllogr. Sect. C* **47,** 2026 (1991).
8. A. C. T. North, D. C. Phillips, and F. S. Mathews, *Acta Crystallogr. Sect. A* **24,** 351 (1968).
9. G. M. Scheldrick, SHELXS86, Program for the Solution of Crystal Structures. University Of Göttingen, Germany, 1986.
10. G. M. Scheldrick, SHELXL93, Program for the Refinement of Crystal Structures. University Of Göttingen, Germany, 1993.
11. C. K. Fair, "MOLEN User's Manual. An Interactive Intelligent System for Crystal Structure Analysis." Enraf-Nonius, Delft, The Netherlands, 1989.
12. C. C. Torardi, *Mater. Res. Bull.* **20,** 705 (1985).
13. I. D. Brown and K. K. Wu, *Acta Crystallogr. Sect. B* **32,** 1957, (1976).
14. J. Vicat, E. Fanchon, P. Strobel, and D. Tran Qui, *Acta Crystallogr. Sect. B* **42,** 162 (1986).
15. R. D. Shannon and C. D. Prewitt, *Acta Crystallogr. Sect. B* **25,** 925 (1969).
16. F. A. Cotton, *Inorg. Chem.* **3,** 1217 (1964).
17. L. Pauling, "Nature of the Chemical Bond," 3rd. ed. Cornell Univ. Press, Ithaca, NY, 1960.
18. R. E. McCarley, *Polyhedron* **5,** 51 (1986).
19. W. H. Mc Carroll, K. Podejko, A. K. Cheetham, D. M. Thomas, and F. DiSalvo, *J. Solid State Chem.* **62,** 241 (1986).
20. S. J. Hibble and I. D. Fawcett, *Inorg. Chem.* **34,** 500 (1995).
21. S. J. Hibble, I. D. Fawcett, and A. C. Hannon, *Acta Crystllogr. Sect. B* **53,** 604 (1997).